

Plastic behavior in shear and degradation of shear modulus of textile composite materials with simple plain weave

Tomáš Kroupa¹, Jan Krystek¹, Hana Srbová¹ & Petr Janda²

Abstract: This work presents results from cyclic tensile tests of thin strips made of three types of textile composite materials with simple plain weave. The materials consist of carbon, aramid and glass fibers, and epoxy matrix. Material axes of specimens form 0°, 45° and 90° angles with the direction of loading force. Subsequently a finite element model is used for identification of material parameters, namely the Young's moduli in directions of principal axes, shear modulus, tensile strengths and shear strength, coefficients of work hardening function and a function of degradation of shear modulus, which depends on level of damage reached.

Keywords: Experiment, Textile composite, Tensile test, Plasticity, Degradation, Shear modulus

1. Introduction

New materials such as composites, piezoelectric materials, rubbers or polymers are used widely in design of structures. Design process is supported by numerical simulations. Accuracy of the simulations depends strongly on capabilities of used material models. Therefore in the field of modeling of composite materials the attention is focused on develop of material models.

This paper deals with develop of material model for textile composites. Van Paeppegem et. al. focused on macro-model with shear elasto-plastic behavior, the new phenomenological model for calculation of shear damage of glass-epoxy textile composite material with plain weave was proposed [1, 2]. Fouinneteau and Pickett [4] improved Ladevèze model [3, 7] using polynomial fit of the damage law. The nonlinear phenomenological model for carbon epoxy composite was proposed in [5] where the influence of the temperature is analyzed. Kroupa et. al. investigated micro- and meso-mechanical models of yarns and textile composites in order to determine elastic material parameters [6].

2. Experiment

Three types of textile composite materials were tested. Materials consist of Aramid (170 gm⁻²), Carbon (160 gm⁻²) or Glass (163 gm⁻²) textiles with simple plain weave and epoxy resin MGS[®] L 285. Epoxy was cured for 2 hours at temperature 50 °C.

Tested strips were subjected to pure tensile and tensile cyclic loading using Zwick/Roell Z050 test machine. Pure tensile test was performed on strips where loading direction forms 0° and 90° angle with 1st principal axis (see Fig. 1). Tensile cyclic test was performed on strips with yarn orientation 45°.

¹ Tomáš Kroupa, Jan Krystek, Hana Srbová,; University of West Bohemia; Faculty of Applied Sciences, Department of mechanics, Univerzitní 8, 306 14, Plzeň, Czech Republic; kroupa@kme.zcu.cz

² Petr Janda; University of West Bohemia, Faculty of Mechanical engineering, Department of Machine design; Univerzitní 8, 306 14, Plzeň, Czech Republic; jandap@kks.zcu.cz

Dimensions of specimens are shown in Fig. 1 together with directions of principal axes, which means directions of the fiber yarns, investigated area, positions of grips and extensometer. If the failure of the material occurred outside the investigated area, the results from this test were omitted. Thicknesses of the specimens are 0.37 mm for Aramid, 0.32 mm for Carbon and 0.25 mm for Glass.

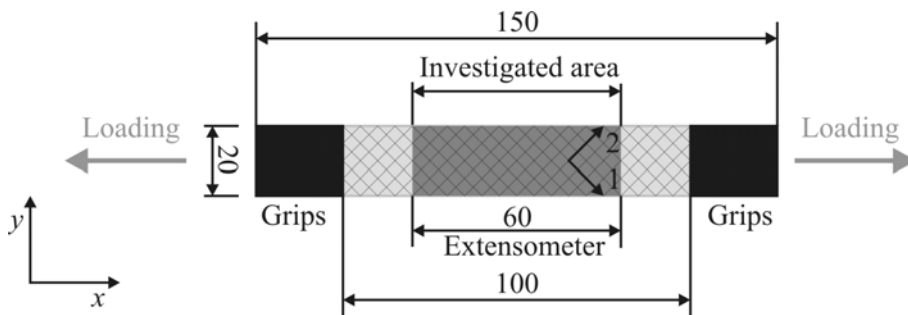


Fig. 1. Dimensions of specimens with depicted principal axes, investigated area and the length of extensometer used in experiments

3. Material model

Numerical model of the strips was meshed using plane stress 4 node elements with 5 mm edge length. The model was fully parameterized using Matlab scripts which generate procedures for MSC.Marc 2010 software with capabilities extended with Fortran subroutines. The whole area between grips was modeled. Nevertheless, only quantities calculated in investigated area were used for identification process.

Finite strain theory was used during the analyses

$$\varepsilon_1 = \frac{\partial u}{\partial x} + \frac{1}{2} \left(\frac{\partial^2 u}{\partial x^2} + \frac{\partial^2 v}{\partial x^2} \right), \quad \varepsilon_2 = \frac{\partial v}{\partial y} + \frac{1}{2} \left(\frac{\partial^2 u}{\partial y^2} + \frac{\partial^2 v}{\partial y^2} \right), \quad (1)$$

$$\gamma_{12} = \left(\frac{\partial u}{\partial y} + \frac{\partial v}{\partial x} \right) + \left(\frac{\partial u}{\partial x} \frac{\partial u}{\partial y} + \frac{\partial v}{\partial x} \frac{\partial v}{\partial y} \right), \quad (2)$$

where x and y are global coordinates, u and v are displacements, and ε_1 , ε_2 and γ_{12} are engineering normal strains and shear strain, respectively.

Generalized Hooke's law with shear damage was used as stress-strain relation

$$\begin{pmatrix} \varepsilon_1 \\ \varepsilon_2 \\ \gamma_{12} \end{pmatrix} = \begin{pmatrix} 1 & -\nu_{12} & 0 \\ E_1 & E_1 & 0 \\ -\nu_{12} & 1 & 0 \\ 0 & 0 & \frac{1}{G_{12}^0(1-d_{12})} \end{pmatrix} \begin{pmatrix} \sigma_1 \\ \sigma_2 \\ \tau_{12} \end{pmatrix}, \quad (3)$$

where E_1 and E_2 are Young's moduli in principal direction 1 and 2 and ν_{12} is Poisson's ratio in plane defined by directions 1 and 2, G_{12}^0 is initial shear modulus in plane 12, and d_{12} is shear damage factor.

Damage factor d_{12} was calculated as a bilinear function of shear failure index

$$d_{12} = A\mathcal{F}_{12} + B \quad \text{for} \quad \mathcal{F}_{12} \in \langle 0, \mathcal{F}_{12}^C \rangle, \quad (4)$$

$$d_{12} = C\mathcal{F}_{12} + D \quad \text{for} \quad \mathcal{F}_{12} \in \langle \mathcal{F}_{12}^C, 1 \rangle, \quad (5)$$

where \mathcal{F}_{12} is shear failure index, \mathcal{F}_{12}^C is critical value of shear failure index. The coefficients A, B, C, D are calculated as

$$A = \mathcal{F}_{12}^C / (1 - \frac{G_{12}^C}{G_{12}^0}), B = 0, C = \frac{G_{12}^C - G_{12}^0}{G_{12}^0(1 - \mathcal{F}_{12}^C)} \text{ and } D = 1 - C - \frac{G_{12}^C}{G_{12}^0}. \quad (6)$$

Failure indices were calculated as square roots of failure indices of Hashin fabric failure criterion (see Table 1).

Table 1. Hashin fabric failure criterion

Tension	Compression	Shear
$\mathcal{F}_1 = \sqrt{\left(\frac{\sigma_1}{X^T}\right)^2 + \left(\frac{\tau_{12}}{S^L}\right)^2}$	$\mathcal{F}_1 = \sqrt{\left(\frac{\sigma_1}{X^C}\right)^2 + \left(\frac{\tau_{12}}{S^L}\right)^2}$	$\mathcal{F}_{12} = \sqrt{\left(\frac{\tau_{12}}{S^L}\right)^2}$
$\mathcal{F}_2 = \sqrt{\left(\frac{\sigma_2}{Y^T}\right)^2 + \left(\frac{\tau_{12}}{S^L}\right)^2}$	$\mathcal{F}_2 = \sqrt{\left(\frac{\sigma_2}{Y^C}\right)^2 + \left(\frac{\tau_{12}}{S^L}\right)^2}$	

Plasticity model was characterized using work hardening function for shear in the form

$$\tau_{12}^y = \frac{G_{12}^0 \varepsilon_p}{\left\{ 1 + \left[\frac{G_{12}^0 \varepsilon_p}{\tau_{12}^0 + \tau_{12}^1 (1 + \tanh(m(\varepsilon_p - \gamma_{12}^0)))} \right]^n \right\}^{\frac{1}{n}}}, \quad (7)$$

where ε_p is equivalent plastic strain, τ_{12}^y is yield stress and the influence of the letter parameters $G_{12}^0, \tau_{12}^0, \tau_{12}^1, m, n$ and γ_{12}^0 on the shape of the work hardening function is shown in the Fig. 2.

4. Identification process

NLPQLP gradient algorithm was used within the identification process. Process was handled using OptiSLang 3.2.0. Objective function (i.e. function which is minimized) consisted from 3 parts. First part was tension curve residual

$$r_t = \sum_{\theta} \sum_{i=1}^N \left(\frac{F^E(\theta, u_i) - F^A(\theta, u_i)}{F_{\max}^E} \right)^2, \quad (8)$$

where the residuum for each yarn angle θ is the difference between force-displacement curves in N points u_i . Superscripts E and A denotes experiment and analysis, respectively, and the meaning of the weighting coefficient F_{\max}^E is described in Fig. 3.

Second part of the total residual was the residual for the tangent of the unload/load cycles

$$r_{ul} = \sum_{i=1}^N \left(\frac{{}^T k^E({}^T u_i) - {}^T k^A({}^T u_i)}{{}^T k^E({}^T u_N) - {}^T k^E({}^T u_1)} \right)^2, \quad (9)$$

where the residual is again summed over the N points and the residual is weighted using the first and last values from the experiment. The idea of determination of the particular values is shown in Fig. 4 and Fig. 5.

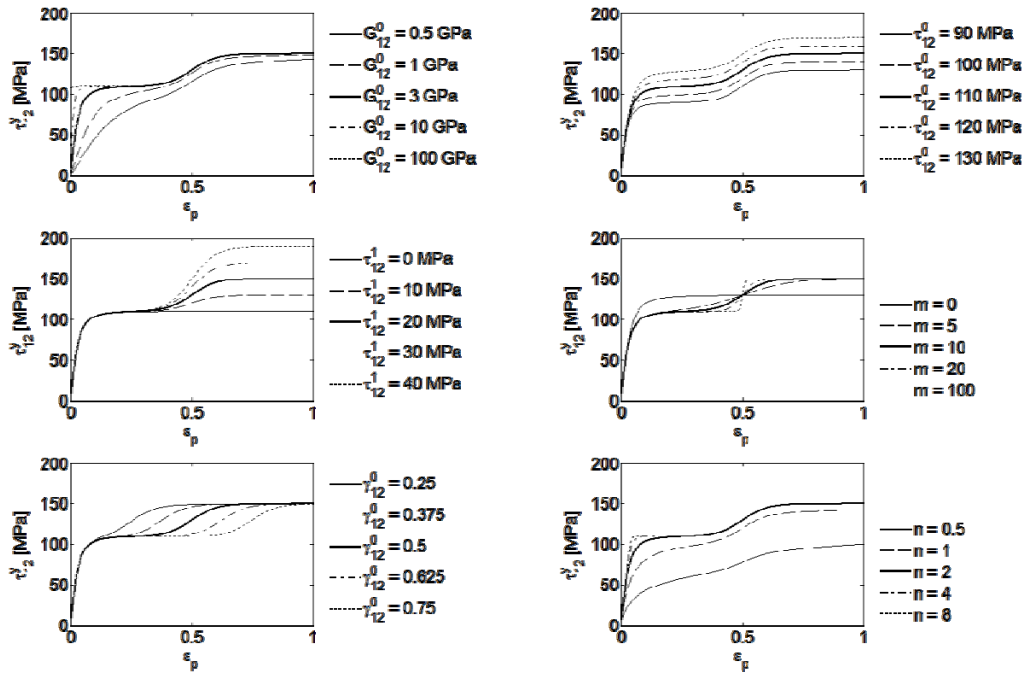


Fig. 2. Influence of each parameter of the work hardening function

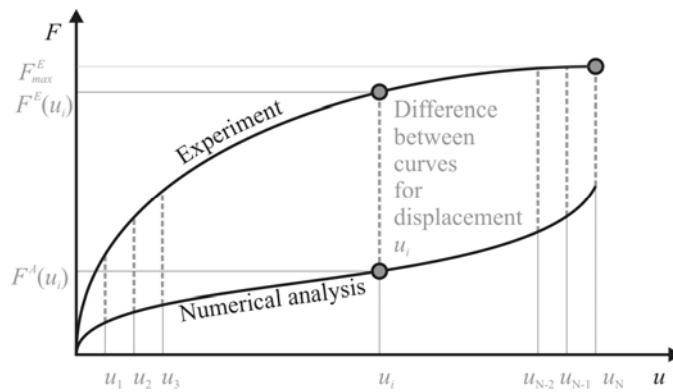


Fig. 3. Scheme of the method for comparing of the force-displacement curves

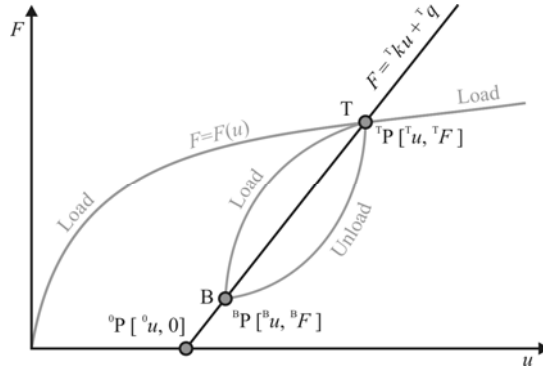


Fig. 4. Tangent of unload/load cycle

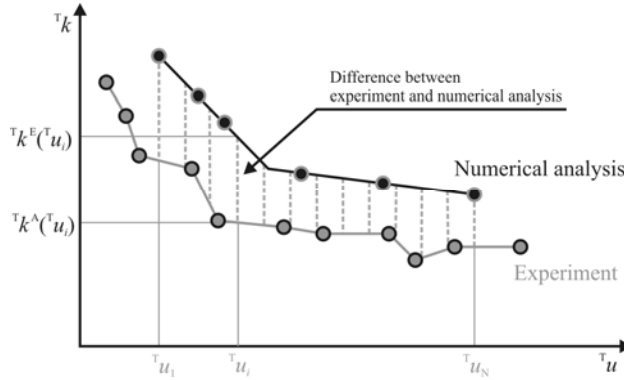


Fig. 5. Comparison of the tangents of the unload/load cycles

The third part of the residual was difference of the maximum failure indices at the ends of the force-displacement curves.

$$r_f = \sum_{\theta} (1 - \max(\mathcal{F}_1(\theta), \mathcal{F}_2(\theta), \mathcal{F}_{12}(\theta)))^2. \quad (10)$$

Total objective function was weighted linear combination of mentioned residuals

$$r = 500 r_t + r_{ul} + 2000 r_f. \quad (11)$$

Number of design necessary to reach the minimum of the residual function was 5694 for aramid textile, 2642 for carbon textile and 3980 for glass textile. The time needed to calculate one design was approx. 1 minute.

5. Results and conclusion

Fig. 6 and Table 2 show the identified results. In all figures is the main force-displacement diagram, which shows tensile curves and unload/load cycles. In the top right corner is the work hardening function, underneath are the failure indices and beneath them is the graph with tangents of the unload/load cycles. Bottom graphs show dependences of the moduli on the failure indices.

The force-displacement curve of the aramid textile, in contrary to the others, shows convex shape of the plastic part of the curve for yarn angle 45° . This is caused by adjusting of the yarns into the direction of loading force.

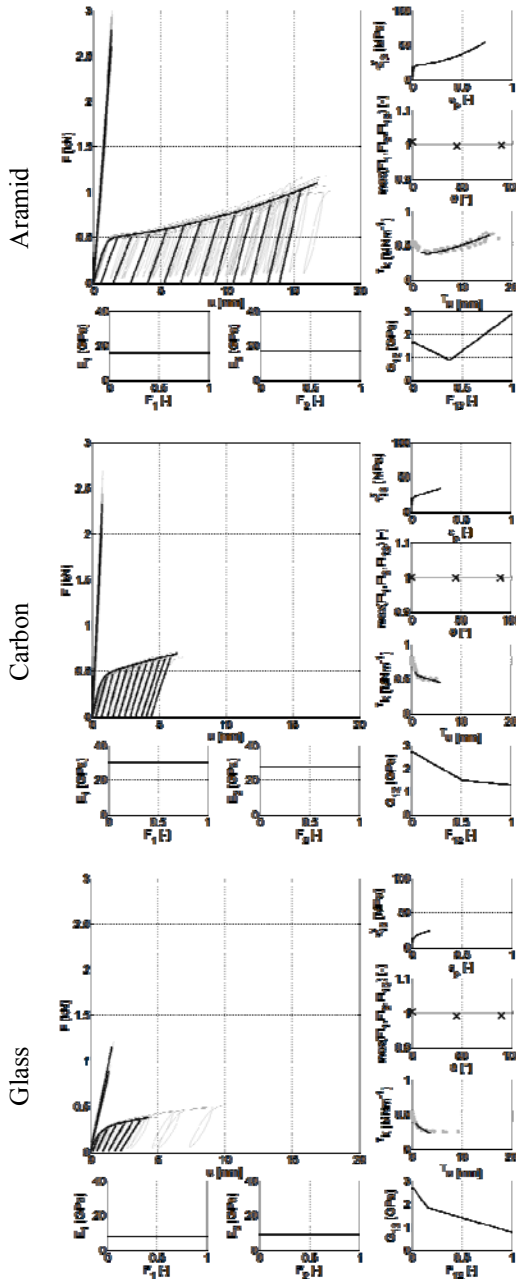


Fig. 6. Results (black – identified results, gray – experiment)

Acknowledgement

This work was supported by projects GAČR GA P101/11/0288, MSM 4977751303 and SGS-2010-046.

The strengths are the highest of all tested materials, nevertheless the Young's moduli are not. The shear modulus is increasing for big plastic strain, this is caused by the change of the directions 1 and 2 of the material. Plastic strain reaches value 0.8.

The strengths X^T and Y^T are similar to aramid, but the shear strength is lower. Young's moduli are highest of all tested materials. Initial shear moduli are almost the same as the value for glass. The decreasing tendency of shear modulus is lower than in the case of glass textile.

The strengths and Young's moduli are lowest of all tested materials. Shear modulus dependence on failure index shows intense decrease. Also the glass textile material is able to sustained the smallest plastic strain of all tested materials.

Table 2. Identified material parameters

Parameter		Aramid	Carbon	Glass	Lower bound	Upper bound
E_1	[GPa]	15.76	30.10	7.77	5.00	40.00
E_2	[GPa]	16.86	27.72	8.81	5.00	40.00
ν_{12}^i	[-]	0.31	0.19	0.24	-	-
G_{12}^0	[GPa]	1.68	2.73	2.73	1.00	3.00
G_{12}^C	[GPa]	0.88	1.48	1.83	0.50	3.00
G_{12}^L	[GPa]	2.86	1.28	0.77	0.50	3.00
\mathcal{F}_{12}^C	[-]	0.38	0.52	0.15	0.05	0.95
m	[-]	1.50	2.00	1.80	1.00	5.00
n	[-]	3.01	1.92	0.89	0.50	4.00
γ_{12}^0	[-]	1.14	0.17	0.12	- 0.50	1.50
X^T	[MPa]	351.75	364.68	178.34	150.00	400.00
$X^{C\text{ii}}$	[MPa]	100.00	100.00	100.00	-	-
Y^T	[MPa]	379.57	324.27	234.14	150.00	400.00
$Y^{C\text{iii}}$	[MPa]	100.00	100.00	100.00	-	-
S^L	[MPa]	98.40	59.23	41.32	30.00	130.00

ⁱ Poisson's ratio was determined using digital image correlation technique [6].

ⁱⁱ Compressive strength in material direction 1 was provided by manufacturer.

ⁱⁱⁱ Compressive strength in material direction 2 was provided by manufacturer.

References

- [1] Van Paepegem W., De Baere I. and Degrieck J., Modeling the nonlinear shear stress-strain response of glass fibre composites. Part I: Experimental results, Elsevier, Composites Science and Technology 66, 2006. pp. 1444-1464, ISSN 0266-3538
- [2] Van Paepegem W., De Baere I. and Degrieck J., Modeling the nonlinear shear stress-strain response of glass fibre composites. Part II: Model development and finite element simulations Elsevier, Composites Science and Technology 66, 2006. pp. 1465-1478, ISSN 0266-3538
- [3] Hochard Ch., Aubourg P.-A., Charles J.-P., Modeling of the mechanical behavior of woven-fabric CFRP laminates up to failure, Elsevier, Composites Science and Technology 61, 2001. pp. 221-230, ISSN 0266-3538
- [4] Founinetau M.R.C., Pickett A.K., Shear mechanism modeling of heavy tow braided composites using a meso-mechanical damage model, Elsevier, Composites Part A: applied science and manufacturing
- [5] Kroupa T., Zemčík R., Klepáček J., Temperature dependence of parameters of non-linear stress-strain relation for carbon epoxy composites, Materials and technology, 2009, vol. 43, no. 2, pp. 69-72, ISSN 1580-2949

- [6] Kroupa T., Janda P., Zemčík R., Linear two scale model for determination of mechanical properties of textile composite material, International conference on materials and technology, Slovenia, Portorož, 2010, ISBN 978-961-92518-2-9
- [7] PAM-crash 2010 solver reference manual, Ladevèze model.